Dalton Transactions

PAPER

View Article Online
View Journal | View Issue

Cite this: *Dalton Trans.*, 2016, **45**, 13742

Supramolecular adducts based on weak interactions between the trimeric Lewis acid complex (perfluoro-*ortho*-phenylene)mercury and polypnictogen complexes†‡

Martin Fleischmann,[a] James S. Jones,[b] Gábor Balázs,[a] François P. Gabbaï*[b] and Manfred Scheer*[a]

Received 22nd June 2016,
Accepted 18th July 2016

DOI: 10.1039/c6dt02507b

www.rsc.org/dalton

Reactions of the trinuclear Lewis acid perfluoro-*ortho*-phenylene)mercury [(*o*-$HgC_6F_4)_3$] (**1**) with the polypnictogen complex [$CpMo(CO)_2(\eta^3\text{-}P_3)$] (**2**) containing a *cyclo*-P_3 ligand and the series of E_2 complexes [$\{CpMo(CO)_2\}_2(\mu,\eta^2\text{:}\eta^2\text{-}E_2)$] (E = P(**3a**), As(**3b**), Sb(**3c**), Bi(**3d**)) are reported. In all cases, the reaction products show very weak interactions between the E_n ligand complexes and the Lewis acid **1**, as evidenced by their highly dynamic behaviour in solution and the formation of adducts in the solid state showing Hg···E contacts below the respective sum of the van der Waals radii. The complexes **2** (P_3), **3a** (P_2) and **3b** (As_2) show interactions of only one pnictogen atom with all three Hg atoms of **1**. The complex **3c** (Sb_2) forms two adducts with **1** showing either a side-on coordination of the Sb_2 dumbbell towards Hg or an end-on coordination of both Sb atoms towards two independent molecules of **1**. The Bi_2 complex **3d** shows an almost parallel alignment of the Bi_2 dumbbell situated above the center of the planar Lewis acid **1**. The arrangements of the E_2 complex series towards **1** are rationalized with the help of electrostatic potential maps obtained by DFT calculations. Finally the structural characterizations of a new modification of the free Sb_2 complex **3c**, the Bi_2 complex **3d**, the starting material of its preparation [$Bi\{CpMo(CO)_3\}_3$] (**4**) and an unprecedented 'Cr_4As_5' cluster **5** are presented.

Introduction

During the last few decades supramolecular chemistry based on weakly interacting molecules instead of strong covalent bonds has gained more and more attention. The investigation of planar electron-deficient molecules has developed into a rich area of research with applications in anion recognition,[1,2] molecular machines,[3] or light emitting materials.[4] In this context, pyridinium cations,[3] or electron deficient aromatic compounds,[1,2] are prototypical representatives. We became particularly interested in the chemistry of the trinuclear organometallic compound (perfluoro-*ortho*-phenylene)-mercury (**1**).[5] Due to its planar geometry this molecule contains three sterically accessible mercury centers whose naturally low Lewis acidity is significantly increased by the fluorinated molecular backbone.[6,7] This unusual Lewis acid builds up alternating binary stacks with aromatic hydrocarbons[8–11] and forms double-sandwich complexes featuring Hg···Cp interactions when reacted with the metallocenes Cp_2Fe and Cp_2Ni (Scheme 1a).[12] Additionally **1** forms weak Lewis acid/base adducts with a variety of O, N and S donors which simultaneously interact with all three Hg atoms (Scheme 1b).[6,7,13] During the past few years we have extended this chemistry to polyphosphorus complexes, observing only weak P···Hg interactions instead of potential Hg···Cp interactions in the reactions of **1** and the triple-decker complex [$(CpMo)_2(\mu,\eta^6\text{:}\eta^6\text{-}P_6)$] (Scheme 1c).[14] Recently we reported the differences in coordination behavior of the aromatic *cyclo*-P_5 and *cyclo*-As_5 ligands from the ferrocene analogues [$Cp^*Fe(\eta^5\text{-}E_5)$] (E = P, As)[15,16] towards the Lewis acid **1**.[17] While the P_5 ring forms a weak Lewis acid/base adduct (Scheme 1d) with one P donor atom, the As_5 ring shows a rather cofacial arrangement towards the molecular plane of **1** with three As atoms interacting simultaneously with the Hg centers (Scheme 1e).

Since the nature of the polypnictogen complexes has been shown to have a dramatic effect on its reactivity towards **1**, we

[a]*Institut für Anorganische Chemie, Universität Regensburg, 93040 Regensburg, Germany. E-mail: manfred.scheer@chemie.uni-regensburg.de; Fax: (+49) 941-943-4439*
[b]*Department of Chemistry, Texas A&M University, College Station, Texas 77843-3255, USA*

† Dedicated to Professor Max Herberhold on the occasion of his 80th birthday.

‡ Electronic supplementary information (ESI) available: Details of syntheses, characterization, X-ray crystallography and DFT calculations. CCDC 1486626–1486635. For ESI and crystallographic data in CIF or other electronic format see DOI: 10.1039/c6dt02507b

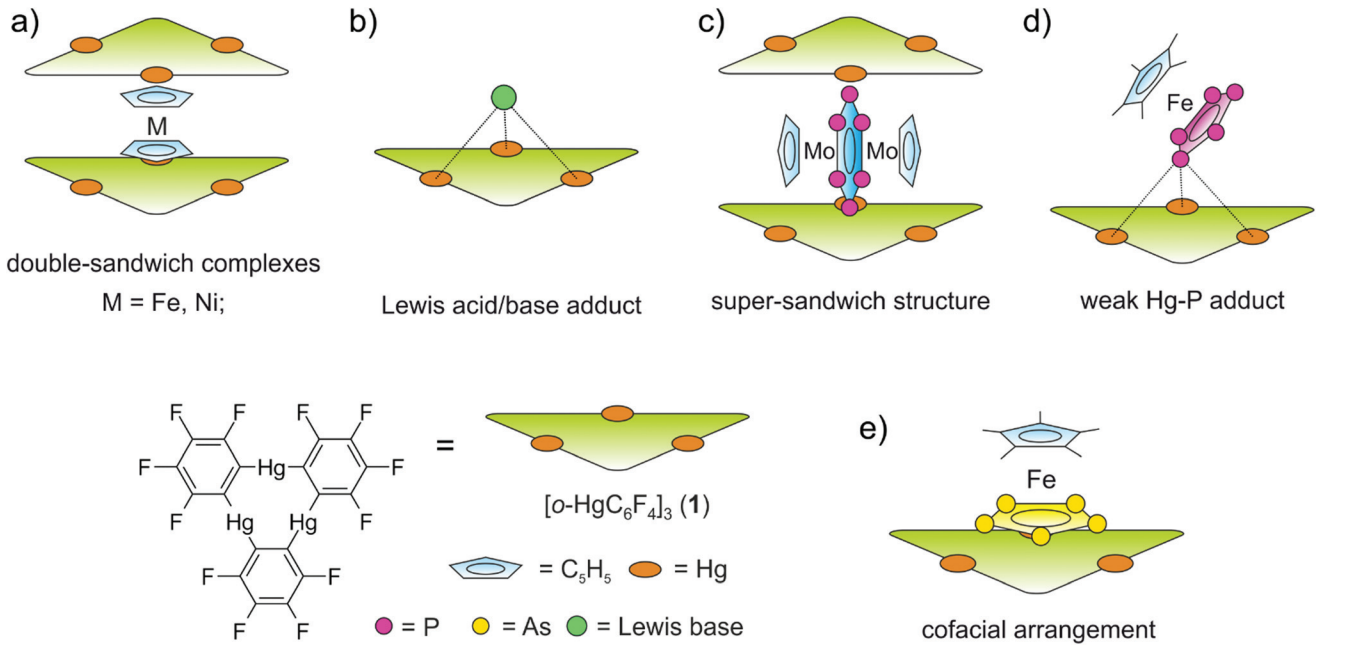

Scheme 1 (a) Representation of the double-sandwich complexes formed from **1** and the metallocenes Cp_2Fe and Cp_2Ni. (b) Illustration of Lewis acid/base adducts of **1** with the Lewis bases simultaneously interacting with all three Hg centers. (c) Super-sandwich structures obtained from **1** and [(CpMo)(μ,η^6:η^6-P_6)]. (d) Coordination of [Cp*Fe(η^5-P_5)] to the three Hg atoms of **1** *via* one P atom. (e) [Cp*Fe(η^5-As_5)] interacting with **1** *via* three As atoms showing an almost cofacial arrangement.

questioned how the trinuclear Lewis acid might interact with a terminal *cyclo*-E_3 ligand and furthermore how its coordination behavior may vary when reacting **1** with complexes of the heavier pnictogen atoms Sb and Bi. To address these questions we first investigated the reactivity of **1** towards the P_3 complex [$CpMo(CO)_2(\eta^3$-$P_3)$] (**2**) and subsequently towards the E_2 complex series [{$CpMo(CO)_2$}$_2$(μ,η^2:η^2-E_2)] E = P(**3a**), As(**3b**), Sb(**3c**), Bi(**3d**) (Scheme 2). For the first time the Bi_2 complex **3d** and the starting material of its synthesis [{$CpMo(CO)_3$}$_3$Bi] (**4**), as well as a new modification of the Sb_2 complex **3c** could be structurally characterized. Additionally, an unprecedented Cr–As cluster [$(CpCr)_4$(μ,η^3:η^3-As_2)(μ,η^3:η^2:η^3-As_3)] (**5**), obtained from a related reaction was also characterized by single crystal X-ray diffraction.

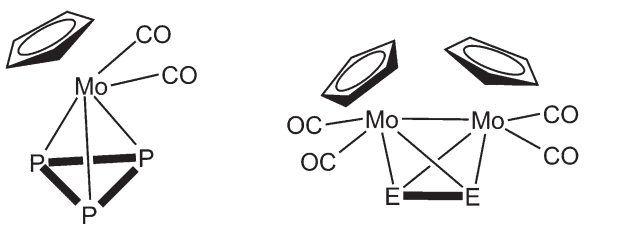

2 E = P(**3a**), As(**3b**), Sb(**3c**), Bi(**3d**)

Scheme 2 Representation of the tetrahedrane complexes [$CpMo(CO)_2(\eta^3$-$P_3)$] (**2**) and [{$CpMo(CO)_2$}$_2$(μ,η^2:η^2-E_2)] (E = P(**3a**), As(**3b**), Sb(**3c**), Bi(**3d**)).

Results and discussion

Syntheses and spectroscopic characterization of the products

The adducts between the pnictogen complexes and **1** are easily prepared by dissolving **1** and an equimolar amount of the *cyclo*-P_3 complex **2** or the E_2 complexes **3a–d** in 10 mL of CH_2Cl_2 until a clear solution is formed. After stirring at room temperature, this solution is filtered and the solvent is removed until the filtrate solution is saturated. Storing the resultant solutions at +4 °C results in product crystallization in a matter of hours to days. Following this approach one can obtain pure samples of equimolar adducts of **1** and the *cyclo*-P_3 complex **2** [(**1**)·(**2**)] (80% isolated yield), the P_2 complex **3a** [(**1**)·(**3a**)] (75%) and the As_2 complex **3b** [(**1**)·(**3b**)] (74%), respectively. In the case of the Sb_2 complex **3c** two adducts with molar ratios of 1 : 1 [(**1**)·(**3c**)] and 2 : 1 [$(\mathbf{1})_2$·(**3c**)] are detected from the same reaction. In the case of the Bi_2 complex **3d** we were able to determine the coexistence of the adduct [(**1**)·$(\mathbf{3d})_2$], pure **1** and pure **3d** next to each other in crystalline form from the same reaction. This observation suggests very weak interactions between **1** and **3d** and prevents a successful separation of these compounds. Moreover, the Sb_2 complex **3c** was isolated in 56% yield after refluxing $(Me_3Si)_2CHSbH_2$ and $CpMo(CO)_3Me$ in xylene for 3 h. The reaction of the triple-decker complex [$(CpCr)_2$(μ,η^5:η^5-As_5)] with **1** enabled the structural characterization of an unprecedented mixed Cr–As cluster **5** (for details see below). Since the described adducts are based on weak Hg···E (E = P, As, Sb, Bi) interactions we assume only very weak association in solution.

In accordance with this, in the mass spectra we never observed any peaks assignable to any adduct but only the starting materials of the described products. The ^{1}H and the ^{19}F NMR spectra in CD_2Cl_2 solution are unchanged compared to the starting compounds. While the $^{31}P\{^{1}H\}$ NMR spectrum of [(**1**)·(**2**)] in CD_2Cl_2 solution shows a sharp singlet at −349.5 ppm which is also unchanged to the starting compound **2** we can observe an upfield shift of about 11 ppm for the singlet of the P_2 ligand **3a** in the case of the adduct [(**1**)·(**3a**)].

Structural characterization of the products in the solid state

General considerations. The solid state structures of the formed adducts exhibit short contacts below the sum of the van der Waals (vdW) radii between pnictogen atoms and the Hg atoms of **1**. The vdW radius of Hg in different compounds is discussed in the literature with reported values ranging from 1.7 Å up to 2.2 Å. In the following discussion the shortest value of 1.7 Å was taken as a reference.[18–23] Therefore, Hg–E distances that are within the sum of the vdW radii of 3.6 Å(P), 3.7 Å(As), 3.9 Å(Sb) or 4.1 Å(Bi) are highlighted by fragmented orange bonds in the following Fig. 1–7.

Crystal structure of the adduct [(1)·(2)]

Fig. 1 shows the solid state structure of the adduct [(**1**)·(**2**)]. Although the symmetry of the *cyclo*-P_3 ligand of complex **2** would generally match the threefold symmetry of the planar Lewis acid **1** it shows a coordination of only one P atom interacting with all three Hg centers of **1**. The resulting Hg–P distances (3.19349(7)–3.25262(6) Å) lie well within the sum of the vdW radii (3.6 Å). These lengths are very comparable to the Hg–P distances found for **1** and $[(CpMo)_2(\mu,\eta^6{:}\eta^6\text{-}P_6)]$ (Scheme 1c), but they are a bit shorter than the closest Hg–P distance that was observed for **1** and $[Cp^*Fe(\eta^5\text{-}P_5)]$ (3.2878(9) Å, Scheme 1d). The angle enclosed between the P_3 plane and the Hg_3 plane measures 65.43(7)°. The P–P bonds show uniform lengths of 2.144(2) Å comparable to the free complex **2**.[24] No Cp–Hg contacts are present.

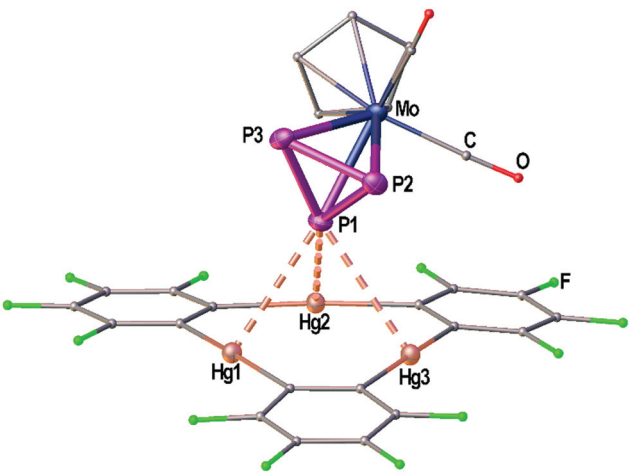

Fig. 1 Solid state structure of compound the adduct [(**1**)·(**2**)]. Selected bond lengths [Å]: Hg1–P1 3.21821(9), Hg2–P1 3.19349(7), Hg3–P1 3.25262(6), P1–P2 2.140(2), P1–P3 2.145(2), P2–P3 2.147(3); interplanar angle P_3 plane – Hg_3 plane = 65.43(7)°. Ellipsoids are drawn at 50% probability. H atoms are omitted and C, F and O atoms are represented as small spheres for clarity.

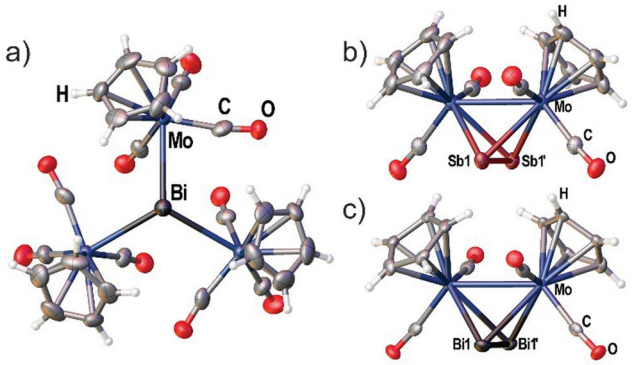

Fig. 2 (a) Crystal structure of $[\{CpMo(CO)_3\}_3Bi]$ (**4**) with viewing direction along the threefold symmetry axis. (b) Crystal structure of the Sb_2 complex **3c**. (c) Crystal structure of the Bi_2 complex **3d**. Selected bond lengths [Å] and angles [°]: **4**: Mo–Bi 3.014(3), angle Mo–Bi–Mo = 113.50(5)°. **3c**: Mo1–Mo1′ 3.1183(10), Sb1–Sb1′ 2.6871(7). **3d**: Mo1–Mo1′ 3.1378(13), Bi1–Bi1′ 2.8580(7). Ellipsoids are drawn at 50% probability for **3c,d** and 30% probability for **4**.

Crystal structures of the Sb_2 complex 3c, the Bi_2 complex 3d and the starting material $[\{CpMo(CO)_3\}_3Bi]$ (4)

Although the synthesis of the Bi_2 complex **3d** was already reported in 1988 the solid state structure was only described of a derivative bearing one methyl group on each Cp ligand.[25,26] During our investigations we were able to determine the solid state structures of **3d** and of the starting material **4** shown in Fig. 2(a) and (c). The synthesis and X-ray structure of the analogous Sb_2 complex **3c** was reported[27] earlier. Moreover, we could structurally characterize a new modification of **3c** by X-ray analysis (see Fig. 2(b)).

The new modification of **3c** crystallizes in the trigonal space group $P3_221$ with half a complex in the asymmetric unit. The complex is crystallographically completed by a twofold rotation axis. The determined bond lengths are in good agreement with the previously determined structure (Mo–Mo 3.114(1) Å, Sb–Sb 2.678(1) Å).

The Bi_2 complex **3d** (see Fig. 2(c)) crystallizes in the monoclinic space group $C2/c$ with half of the complex in the asymmetric unit. The Mo–Mo bond as well as the Bi–Bi bond is bisected by the twofold rotation axis. The Bi–Bi bond length of 2.8580(7) Å is very comparable to the 2.838(1) Å found for $[\{(\eta^5\text{-}C_5H_4Me)Mo(CO)_2\}_2(\mu,\eta^2{:}\eta^2\text{-}Bi_2)]$.[25,26]

Compound **4** crystallizes in the trigonal space group $P31c$ with the central Bi atom situated on the threefold rotation axis (see Fig. 2a) showing a Mo–Bi bond length of 3.014(3) Å. The bonding environment around Bi is best described as trigonal pyramidal with the three Mo–Bi–Mo angles summing up to 340.50(5)°.

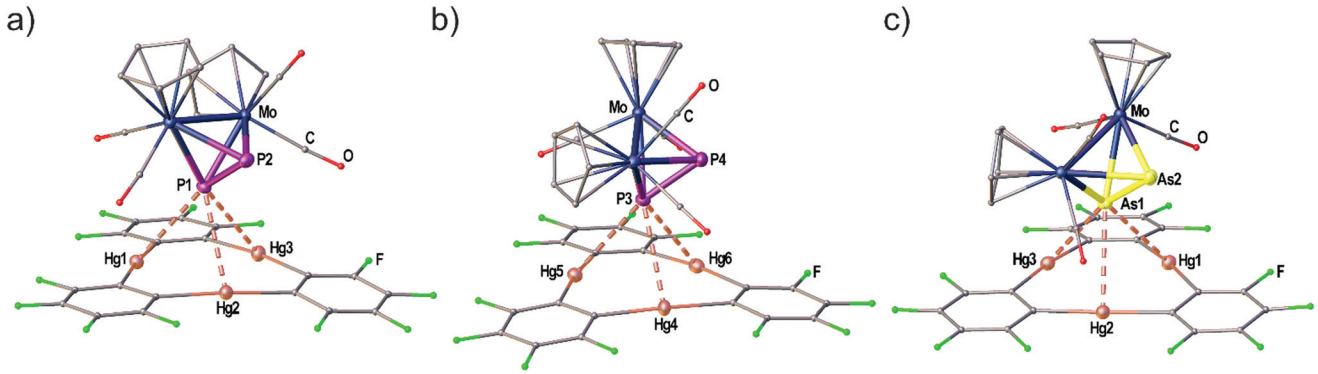

Fig. 3 Independent molecules A (a) and B (b) found in the solid state structure of the adduct [(**1**)·(**3a**)]. (c) Crystal structure of the adduct [(**1**)·(**3b**)]. Selected bond lengths [Å]: [(**1**)·(**3a**)]: Hg1–P1 3.1040(2), Hg1–P2 3.3369(2), Hg1–P3 3.1953(2), Hg4–P3 3.3557(2), Hg5–P3 3.1609(2), Hg6–P3 3.2299(2), P1–P2 2.0883(1), P3–P4 2.0948(1). [(**1**)·(**3b**)]: Hg1–As1 3.2702(2), Hg2–As1 3.3259(1), Hg3–As1 3.3788(2), As1–As2 2.3162(1). Angles of E_2 dumbbells to Hg_3 plane: P1P2–Hg1Hg2Hg3 36.33(1)°, P3P4–Hg4Hg5Hg6 38.05(1)°, As1As2–Hg1Hg2Hg3 37.00(1)°. Ellipsoids are drawn at 50% probability. H atoms are omitted and C, F and O atoms are represented as small spheres for clarity.

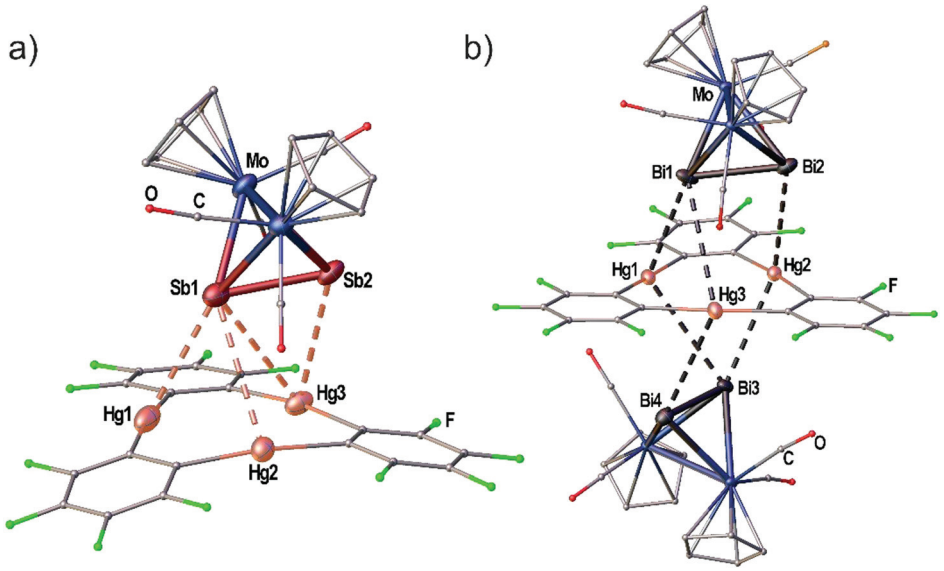

Fig. 4 (a) Solid state structure of the adduct [(**1**)·(**3c**)]. (b) Solid state structure of the adduct [(**1**)·(**3d**)$_2$]. Selected bond lengths [Å]: [(**1**)·(**3c**)]: Hg1–Sb1 3.4336(1), Hg2–Sb1 3.8621(1), Hg3–Sb1 3.7879(2), Hg3–Sb2 3.5222(1), Sb1–Sb2 2.6914(1). [(**1**)·(**3d**)$_2$]: Hg1–Bi1 3.4859(1), Hg2–Bi2 3.6370(1), Hg3–Bi1 4.0481(2), Bi1–Bi2 2.8479(1), Hg1–Bi3 3.9046(1), Hg2–Bi3 3.5888(1), Hg3–Bi4 3.7827(1), Bi3–Bi4 2.8537(1). Ellipsoids are drawn at 50% probability. H atoms are omitted and C, F and O atoms are represented as small spheres for clarity. Angles E_2 straight to Hg_3 plane: Sb1Sb2–Hg1Hg2Hg3 7.03(1)°, Bi1Bi2–Hg1Hg2Hg3 5.72(1)°, Bi3Bi4–Hg1Hg2Hg3 2.50(1)°.

Structural characterization of the adducts formed from 1 and the E_2 complexes 3a–d

The adduct [(**1**)·(**3a**)] crystallizes in the triclinic space group $P\bar{1}$ with two independent formula units [(**1**)·(**3a**)] in the asymmetric unit shown in Fig. 3(a) and (b). Both molecules of **3a** interact with all three Hg atoms of the Lewis acid **1** *via* one P atom which is situated above the center of **1** while the other P atom shows no Hg···P contacts. The resulting Hg–P distances lie in the range of 3.10401(15)–3.3557(2) Å. The P–P bond lengths are not affected in comparison to free **3a** (2.079(2) Å)[28] by the coordination. The angles between the direction of the P_2 dumbbell and the Hg_3 plane measure 36.33(1)° (P1–P2) and 38.05(1)° (P3–P4), respectively.

When looking at the As_2 complex **3b** and its interaction with **1** in the solid state shown in Fig. 3(c) it can be noted that the assembly in the adduct [(**1**)·(**3b**)] is very similar to the P_2 complex **3a**. This observation was very surprising since we previously observed a distinctly different assembly of *cyclo*-P_5 and *cyclo*-As_5 ligands with **1** (see Scheme 1(d) and (e)). The compound [(**1**)·(**3b**)] crystallizes in a different unit cell (but same space group $P\bar{1}$) than [(**1**)·(**3a**)] containing only one formula unit in the asymmetric unit. The As_2 complex **3b** is interacting with all three Hg atoms of the Lewis acid **1** *via* one As atom

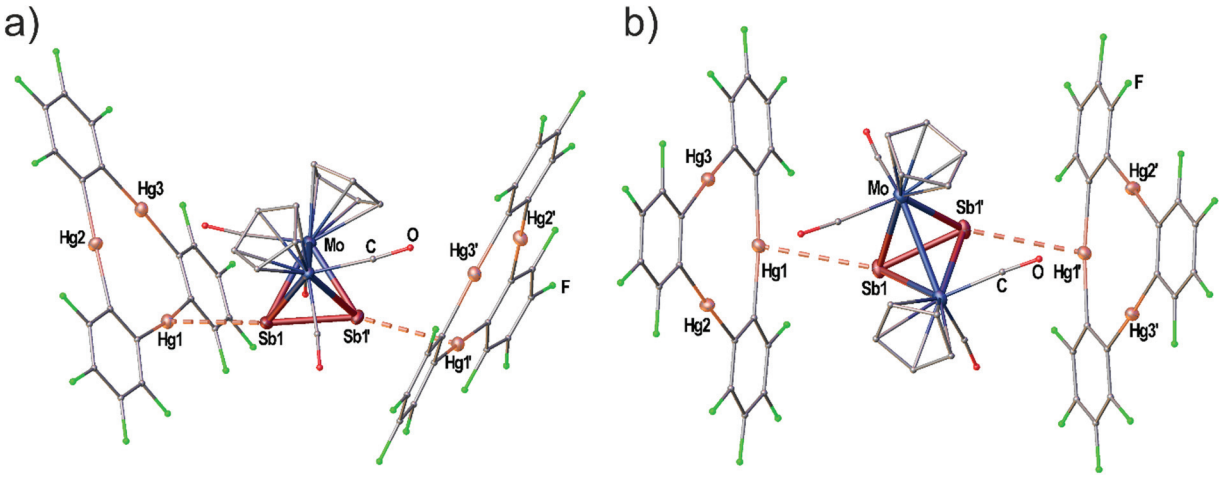

Fig. 5 Solid state structure of the adduct $[(\mathbf{1})_2\cdot(\mathbf{3c})]$. (a) Viewing direction along the Mo–Mo bond. (b) Viewing direction along the crystallographic *b*-axis (twofold rotation axis). Selected bond lengths [Å]: Hg1–Sb1 3.5283(9), Sb1–Sb1′ 2.6863(13). Ellipsoids are drawn at 50% probability. H atoms are omitted and C, F and O atoms are represented as small spheres for clarity.

while the second As atom does not show any Hg···As contacts. The resulting Hg–As distances lie in the range of 3.27021(13)–3.37875(13) Å and are well within the sum of the vdW radii for Hg and As (3.7 Å). The As–As bond length is 2.31607(10) Å long which is essentially unchanged to free **3b** (2.305(3) Å).[29] The angle enclosed by the As_2 dumbbell and the Hg_3 plane (37.00(1)°) also compares very well to the analogous P_2 adduct.

When the Sb_2 complex **3c** is allowed to react with the Lewis acid **1** two sorts of crystals (orange and red) are formed from the same solution. Single crystal X-ray diffraction analysis revealed that the orange crystals consist of the equimolar adduct of **1** and **3c** $[(\mathbf{1})\cdot(\mathbf{3c})]$ depicted in Fig. 4a. For E = Sb, the assembly of the Mo_2E_2 complex is different from E = P, As. The most apparent distinction is the angle enclosed by the E_2 dumbbell and the Hg_3 plane in $[(\mathbf{1})\cdot(\mathbf{3c})]$ which measures only 7.03(1)°. Although Sb1 is also situated above the center of **1** the resulting Hg–Sb distances differ significantly. The shortest distance is observed for Hg1–Sb1 with 3.4336(1) Å while the distances to Hg2 and Hg3 are almost at the edge of vdW contacts (3.9 Å). The observed arrangement of **1** and **3c** shows one additional Hg-Sb contact between Sb2 and Hg3 with 3.5222(1) Å and can be described as a side-on coordination of the Sb–Sb bond to Hg3. The Sb–Sb bond length of 2.6914(1) Å is essentially unchanged compared to free **3c** (*vide supra*).[27] X-ray analysis of the red crystals from the same reaction consist of the adduct $[(\mathbf{1})_2\cdot(\mathbf{3c})]$ where one Sb_2 complex **3c** is surrounded by two molecules of the Lewis acid **1** depicted in Fig. 5(a). The Sb atom Sb1 shows only one contact to Hg1 with 3.5283(9) Å. The adduct $[(\mathbf{1})_2\cdot(\mathbf{3c})]$ crystallizes in the monoclinic space group *P*2/*n*. The twofold rotation axis bisects the Mo–Mo bond as well as the Sb–Sb bond of **3c** (see Fig. 5b). The angle enclosed by both Hg_3 planes amounts to 53.45(1)°. The Sb1–Sb1′ bond length of 2.6863(13) Å is consistently unchanged compared to free **3c**.

When the reactivity of the Bi_2 complex **3d** towards the Lewis acid **1** was investigated by using different stoichiometries, black crystals of pure **3d**, colorless crystals of pure **1** and black crystals of the adduct $[(\mathbf{1})\cdot(\mathbf{3d})_2]$ were obtained next to each other from one reaction. Although numerous crystals were mounted it was not possible to identify any adducts of **1** and **3d** in different molar ratios. The solid state structure of $[(\mathbf{1})\cdot(\mathbf{3d})_2]$ is depicted in Fig. 4(b). The compound crystallizes in the triclinic space group $P\bar{1}$ with two units of **3d** interacting with one molecule of the Lewis acid **1** from both sides *via* both Bi atoms in the asymmetric unit. The Bi–Bi dumbbells are arranged almost parallel to the Hg_3 plane with enclosed angles of 2.50(1)° and 5.72(1)°, respectively. The center of **1** is not situated below one of the Bi atoms but rather the middle of the Bi–Bi bonds. The resulting Hg–Bi distances vary significantly in the range of 3.48590(8)–4.04806(13) Å. The Bi–Bi bond lengths in the adduct $[(\mathbf{1})\cdot(\mathbf{3d})_2]$ are essentially identical to the free complex **3d** (*vide supra*).[25,26]

In order to aid in the rationalization of the observed structural trends for the adducts between **3a–3d** and **1**, their constituent compounds were optimized by density functional theory (DFT) methods. The large computed HOMO–LUMO gaps between **1** and **3a–d** of 3.06, 3.00, 2.88, and 2.74 eV, respectively, suggest that orbital-based interactions are not likely to be dominant within the pnictogen-mercury bonding found in these adducts. Instead, similar to the related adducts of **1** with the *cyclo*-P_5 and *cyclo*-As_5 rings of $[Cp^*Fe(\eta^5\text{-}E_5)]$ complexes,[17] electrostatic and dispersion forces are likely to factor strongly in the stabilization of the observed structures. In order to probe the potential role of electrostatic forces in the observed adducts, we inspected the electrostatic potential maps of the constituent complexes shown in Fig. 6. In both **3a** and **3b**, the electrostatic potential surface shows accumulation of negative character both across the length of the E–E bond and at the phosphorus and arsenic termini. For the electrostatic potential map of complex **3c**, negative character is preferentially accumulated at the Sb–Sb bond, with modest negative character still present at the Sb termini. Finally, in the electrostatic

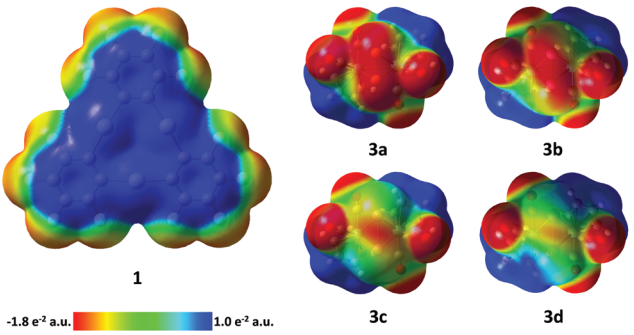

Fig. 6 Electrostatic potential surfaces of compounds **1** and **3a–d** (isovalue = 0.004). **3a–d**: viewing direction along the C_2 axis of the complexes. E_2 bonds are in front.

potential map of complex **3d**, negative character is expressed almost exclusively at the Bi–Bi bond. Taken together, these results suggest that in adducts of **1** with **3a** and **3b**, the surfaces of the pnictogen termini are complimentary with the positive surface of the mercury centers in **1**. Complex **3c** appears to be a borderline case, with both residual negative character at the Sb termini and increasing preference for negative character accumulation at the Sb–Sb bond possibly accounting for the two distinctly different modes which can be observed in the two adducts of **1** and **3c**. Finally, the lack of negative character at the Bi termini in complex **3d** accounts for the observed side-on binding mode, as the surface of the Bi–Bi bond is most complimentary with the positive character found at the mercury surfaces in **1**. In an effort to gain further insight into the nature of the E–Hg interactions, adducts [(**1**)·(**3a**)], [(**1**)·(**3b**)], [(**1**)$_2$·(**3c**)], [(**1**)·(**3c**)], and [(**1**)·(**3d**)$_2$] were subjected to QTAIM[30] analysis at their crystal structure geometries (see ESI‡ for details). In all cases, bond critical points (BCPs) were found between the pnictogen atoms of **3a–d** and the mercury atoms of **1**. Additional intermolecular BCPs were found between the oxygen atoms of the carbonyl ligands of **3a–d** and the mercury and carbon atoms of **1**. Inspection of the features of the electron density distribution function ($\rho(r)$) at the intermolecular BCPs found that similar to the previously observed adducts of **1** with the *cyclo*-P_5 and *cyclo*-As_5 rings of [Cp*Fe(η^5-E_5)] complexes, electrostatic and dispersion forces predominate in the adducts of **3a–d** with **1**.

Structural characterization of the adduct [(**1**)$_2$·(**5**)] and the 'Cr_4As_5' cluster **5**

The Cr–As cluster **5** was characterized by chance when [(CpCr)$_2$(μ,η^5:η^5-As_5)][31] was reacted with **1**. The reaction conducted at room temperature resulted in the formation of amorphous black powder which could not be further characterized and a few dark green crystals of the adduct [(**1**)$_2$·(**5**)]. The solid state structure of [(**1**)$_2$·(**5**)] is depicted in Fig. 7(a) showing the unprecedented 'Cr_4As_5' cluster **5** surrounded by two molecules of **1**. The adduct [(**1**)$_2$·(**5**)] crystallizes in the monoclinic space group *C*2/*c* with the twofold rotation axis running through As3 as well as the middle of the As1–As1′ bond. The Hg_3 planes of the two molecules of **1** are arranged almost perpendicular to each other with an enclosed angle of 87.36(1)°. The assembly results in eight Hg–As distances below the sum of the vdW radii (3.7 Å). The cluster core of **5** depicted in Fig. 7(b) consists of four Cr atoms in a butterfly structure with Cr–Cr bond lengths of 2.9075(1)–3.0134(1) Å, one As_2 ligand and one As_3 ligand. There is a η^5-bound Cp ligand on each Cr atom. Since the Lewis acid **1** generally shows the formation of weakly interacting adducts in combination with pnictogen donors[14,17] (see above) without changing the geometry or composition of the reactants we assume that the unprecedented cluster **5** was an impurity of the used [(CpCr)$_2$(μ,η^5:η^5-As_5)] sample that could not be separated by chromatography before (most probably formed as a byproduct in the thermolytic synthesis of [(CpCr)$_2$(μ,η^5:η^5-As_5)]).[31] The cluster could presumably only be characterized by

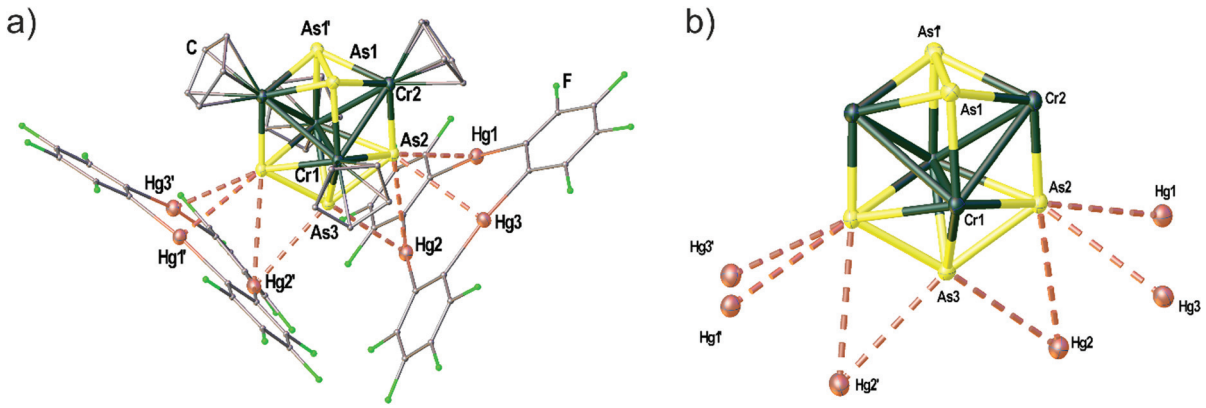

Fig. 7 Solid state structure of the adduct [(**1**)$_2$·(**5**)]. (a) Representation of the Cr–As cluster **5** coordinated by two molecules of **1**. (b) Illustration of the central cluster core of **5** omitting the four Cp ligands on Cr and only showing the contacts to the Hg atoms of **1**. Selected bond lengths [Å]: Hg1–As2 2.6863(1), Hg2–As2 3.6066(1), Hg2–As3 3.3557(1), Hg3–As2 3.3944(1), As1–As1′ 2.4922(1), As2–As3 2.4456(1), Cr1–Cr1′ 2.9075(1), Cr1–Cr2 2.9453(1), Cr1–Cr2′ 3.0134(1), Cr1–As1 2.5067(1), Cr1–As2 2.5899(1), Cr1–As2′ 2.5698(1), Cr1–As3 2.4683(1), Cr2–As1 2.4450(1), Cr2–As1′ 2.4380(1), Cr2–As2 2.3604(1); angle Hg_3 plane – Hg_3 plane 87.36(1)°. Ellipsoids are drawn at 50% probability. H atoms are omitted and C, F and O atoms are represented as small spheres for clarity.

X-ray diffraction as it crystallizes very well in the adduct with **1** due to the stabilization by several Hg···As contacts in the solid state. Unfortunately, **5** could not be further characterized due to the very low yield of this side-product.

Conclusion

The presented results demonstrate the facile preparation of adducts starting from the planar Lewis acid **1** and polypnictogen complexes. While the interactions of the Hg atoms of **1** and the pnictogen donors are very weak resulting in dissociation in solution, several contacts below the sum of the vdW radii can be observed in the solid state. Here, the polyphosphorus complexes **2** (P_3) and **3a** (P_2) show interaction of only one P atom with all three Hg atoms of **1** in accordance with previously described results from reactions of *cyclo*-P_5 and *cyclo*-P_6 complexes with **1**. In the series of the E_2 complexes **3a–d** a significant influence of the pnictogen atom (E = P, As, Sb, Bi) is revealed. While the assembly of the As_2 complex **3b** is very similar to its P analogue, a different mode of aggregation was observed for the Sb_2 and Bi_2 complexes **3c** and **3d**. In case of **3c** the formation of two adducts with **1** was detected. Therein, **3c** shows two distinctly different coordination modes towards the planar Lewis acid **1**. The Sb_2 ligand either shows a side-on arrangement towards one molecule of **1** or an end-on coordination of both Sb atoms towards two independent molecules of **1**. In contrast, the Bi_2 complex **3d** shows an almost parallel alignment of the Bi_2 dumbbell situated above the center of the planar Lewis acid **1**. The isolation of [(**1**)·(**3d**)$_2$] does not only represent the first adduct of **1** with a Bi based Lewis base, but is also the first follow-up chemistry that has been described for the Bi_2 complex **3d**. The observed arrangements of the E_2 complex series can be well rationalized by analysis of the electrostatic potential maps of the complexes **3a–d**. In addition, QTAIM analysis and direct comparison to the previously described adducts of **1** and the *cyclo*-P_5 and *cyclo*-As_5 ligands of [Cp*Fe(η^5-E_5)] complexes suggest that electrostatic and dispersion forces predominate in the adducts of **3a–d** with **1**. Finally, the structural characterization of a new modification of the Sb_2 complex [{CpMo(CO)$_2$}$_2$(μ,η^2:η^2-Sb_2)] (**3c**), the Bi_2 complex [{CpMo(CO)$_2$}$_2$(μ,η^2:η^2-Bi_2)] (**3d**), the starting material [{CpMo(CO)$_3$}$_3$Bi] (**4**), and a novel [(CpCr)$_4$As$_5$] cluster **5** are presented.

Acknowledgements

Manfred Zabel is acknowledged for recording the X-ray dataset for **3c**. This work was financially supported by the Deutsche Forschungsgemeinschaft, the National Science Foundation (CHE-1300371) and the Welch Foundation (A-1423). Texas A&M University (Arthur E. Martell Chair of Chemistry) and the Laboratory for Molecular Simulation at Texas A&M University (computational resources) are gratefully acknowledged.

Notes and references

1 B. L. Schottel, H. T. Chifotides and K. R. Dunbar, *Chem. Soc. Rev.*, 2008, **37**, 68–83.
2 B. P. Hay and V. S. Bryantsev, *Chem. Commun.*, 2008, 2417–2428.
3 J. F. Stoddart, *Chem. Soc. Rev.*, 2009, **38**, 1802–1820.
4 M. A. Omary, R. M. Kassab, M. R. Haneline, O. Elbjeirami and F. P. Gabbaï, *Inorg. Chem.*, 2003, **42**, 2176–2178.
5 P. Sartori and A. Golloch, *Chem. Ber.*, 1968, **101**, 2004–2009.
6 M. R. Haneline, R. E. Taylor and F. P. Gabbaï, *Chem. – Eur. J.*, 2003, **9**, 5188–5193.
7 T. J. Taylor, C. N. Burress and F. P. Gabbaï, *Organometallics*, 2007, **26**, 5252–5263.
8 M. Tsunoda and F. P. Gabbaï, *J. Am. Chem. Soc.*, 2000, **122**, 8335–8336.
9 C. N. Burress, M. I. Bodine, O. Elbjeirami, J. H. Reibenspies, M. A. Omary and F. P. Gabbaï, *Inorg. Chem.*, 2007, **46**, 1388–1395.
10 M. R. Haneline, M. Tsunoda and F. P. Gabbaï, *J. Am. Chem. Soc.*, 2002, **124**, 3737–3742.
11 I. A. Tikhonova, D. A. Gribanyov, K. I. Tugashov, F. M. Dolgushin, A. S. Peregudov, D. Y. Antonov, V. I. Rosenberg and V. B. Shur, *J. Organomet. Chem.*, 2010, **695**, 1949–1952.
12 M. R. Haneline and F. P. Gabbaï, *Angew. Chem., Int. Ed.*, 2004, **43**, 5471–5474.
13 M. C. Ball, D. S. Brown, A. G. Massey and D. A. Wickens, *J. Organomet. Chem.*, 1981, **206**, 265–277.
14 M. Fleischmann, C. Heindl, M. Seidl, G. Balázs, A. V. Virovets, E. V. Peresypkina, M. Tsunoda, F. P. Gabbaï and M. Scheer, *Angew. Chem., Int. Ed.*, 2012, **51**, 9918–9921.
15 O. J. Scherer and T. Brück, *Angew. Chem., Int. Ed.*, 1987, **26**, 59–59.
16 O. J. Scherer, C. Blath and G. Wolmershäuser, *J. Organomet. Chem.*, 1990, **387**, C21–C24.
17 M. Fleischmann, J. S. Jones, F. P. Gabbaï and M. Scheer, *Chem. Sci.*, 2015, **6**, 132–139.
18 A. J. Canty and G. B. Deacon, *Inorg. Chim. Acta*, 1980, **45**, L225–L227.
19 S. S. Batsanov, *J. Chem. Soc., Dalton Trans.*, 1998, 1541–1546.
20 P. Pyykko and M. Straka, *Phys. Chem. Chem. Phys.*, 2000, **2**, 2489–2493.
21 K. R. Flower, V. J. Howard, S. Naguthney, R. G. Pritchard, J. E. Warren and A. T. McGown, *Inorg. Chem.*, 2002, **41**, 1907–1912.
22 A. F. Holleman, E. Wiberg and N. Wiberg, *Lehrbuch der Anorganischen Chemie*, Walter de Gruyter, Berlin, 2007.
23 It should be noted, that the CCDC take 1.55 Å as the vdW radius of Hg (taken from: A. Bondi, *J. Phys. Chem.*, 1964, **68**, 441), but this value is probably too small since the authors already mention the fact that it is uncertain how to

estimate the vdW radius of metals in organometallic compounds.
24 O. J. Scherer, H. Sitzmann and G. Wolmershäuser, *Acta Crystallogr., Sect. C: Cryst. Struct. Commun.*, 1985, **41**, 1761–1763.
25 W. Clegg, N. A. Compton, R. J. Errington and N. C. Norman, *Polyhedron*, 1988, **7**, 2239–2241.
26 W. Clegg, N. A. Compton, R. J. Errington, G. A. Fisher, N. C. Norman and T. B. Marder, *J. Chem. Soc., Dalton Trans.*, 1991, 2887–2895.
27 J. R. Harper and A. L. Rheingold, *J. Organomet. Chem.*, 1990, **390**, C36–C38.
28 O. J. Scherer, H. Sitzmann and G. Wolmershäuser, *J. Organomet. Chem.*, 1984, **268**, C9–C12.
29 P. J. Sullivan and A. L. Rheingold, *Organometallics*, 1982, **1**, 1547–1549.
30 R. F. W. Bader, *Atoms in Molecules: A Quantum Theory*, Cambridge University Press, Oxford, UK, 1991.
31 O. J. Scherer, W. Wiedemann and G. Wolmershäuser, *J. Organomet. Chem.*, 1989, **361**, C11–C14.